Cell

Resource

Ubiquitin Chain Editing Revealed by Polyubiquitin Linkage-Specific Antibodies

Kim Newton,[1] Marissa L. Matsumoto,[2] Ingrid E. Wertz,[3] Donald S. Kirkpatrick,[4] Jennie R. Lill,[4] Jenille Tan,[1] Debra Dugger,[1] Nathaniel Gordon,[2,6] Sachdev S. Sidhu,[2,7] Frederic A. Fellouse,[2,8] Laszlo Komuves,[5] Dorothy M. French,[5] Ronald E. Ferrando,[5] Cynthia Lam,[3] Deanne Compaan,[3,9] Christine Yu,[3] Ivan Bosanac,[3] Sarah G. Hymowitz,[3] Robert F. Kelley,[2] and Vishva M. Dixit[1,*]

[1]Department of Physiological Chemistry
[2]Department of Antibody Engineering
[3]Department of Protein Engineering
[4]Department of Protein Chemistry
[5]Department of Pathology
Genentech, Inc., 1 DNA Way, South San Francisco, CA 94080, USA
[6]Present address: Ammunix, Inc., 500 Ellis Street, Suite B, Mountain View, CA 94043, USA
[7]Present address: Terrence Donnelly Centre for Cellular and Biomolecular Research, Banting and Best Department of Medical Research, University of Toronto, 160 College Street, Toronto, Ontario M5S 3E1, Canada
[8]Present address: Samuel Lunenfeld Research Institute, Mount Sinai Hospital, 600 University Avenue, Toronto, Ontario M5G 1X5, Canada
[9]Present address: General Biologic, 169 Mengzi Road, Suite 301, Building 2, Shanghai, 200023 PR China
*Correspondence: dixit@gene.com
DOI 10.1016/j.cell.2008.07.039

SUMMARY

Posttranslational modification of proteins with polyubiquitin occurs in diverse signaling pathways and is tightly regulated to ensure cellular homeostasis. Studies employing ubiquitin mutants suggest that the fate of polyubiquitinated proteins is determined by which lysine within ubiquitin is linked to the C terminus of an adjacent ubiquitin. We have developed linkage-specific antibodies that recognize polyubiquitin chains joined through lysine 63 (K63) or 48 (K48). A cocrystal structure of an anti-K63 linkage Fab bound to K63-linked diubiquitin provides insight into the molecular basis for specificity. We use these antibodies to demonstrate that RIP1, which is essential for tumor necrosis factor-induced NF-κB activation, and IRAK1, which participates in signaling by interleukin-1β and Toll-like receptors, both undergo polyubiquitin editing in stimulated cells. Both kinase adaptors initially acquire K63-linked polyubiquitin, while at later times K48-linked polyubiquitin targets them for proteasomal degradation. Polyubiquitin editing may therefore be a general mechanism for attenuating innate immune signaling.

INTRODUCTION

Ubiquitination is a reversible, ATP-dependent posttranslational modification in which the C-terminal glycine of ubiquitin is covalently linked through an isopeptide bond to the side chain of a lysine or, less commonly, the amino terminus of a target protein. Three classes of enzymes are required: the ubiquitin-activating E1, an ubiquitin-conjugating E2, and an ubiquitin ligase E3. The E3s select the substrate to be modified. A polyubiquitin chain is formed when one of the seven lysine side chains within ubiquitin is linked to the C-terminal glycine of another ubiquitin. The best characterized linkages to date utilize ubiquitin K48 and K63. K48-linked polyubiquitin predominantly, but not exclusively, targets proteins for proteasomal degradation, whereas K63-linked polyubiquitin more often regulates protein function, subcellular localization, or protein-protein interactions. Ubiquitination is reversible due to deubiquitinating enzymes (DUBs) that can cleave ubiquitin from modified proteins (Hershko and Ciechanover, 1998).

Identification of polyubiquitin chain linkages on modified proteins has relied largely on mass spectrometry (Kirkpatrick et al., 2006) and/or the use of mutant ubiquitins with one or more lysines mutated to arginine (Ea et al., 2006; Finley et al., 1994; Spence et al., 1995; Wang et al., 2001; Wertz et al., 2004). Both approaches have their disadvantages. Mass spectrometry is labor intensive, requires sophisticated instrumentation, and has limited sensitivity when interrogating rapid changes in the ubiquitination status of endogenous proteins. Overexpressing mutant ubiquitins in cells or using mutant ubiquitins in vitro may not recapitulate accurately modifications that involve wild-type, endogenous ubiquitin. We have addressed this barrier to progress by developing linkage-specific antibodies with utility in a broad range of applications including immunoprecipitation (IP), immunofluorescence, immunohistochemistry, and western blotting. Given that ubiquitination is emerging as a critical regulator of a variety of cellular processes including, but not limited to, cell-cycle progression, the DNA-damage response, activation of transcription by NF-κB, and regulation of cell survival (Hershko and Ciechanover, 1998), these reagents hold the

same potential as antibodies specific for phosphorylated amino acids in revealing the rapid changes in posttranslational modifications that accompany signaling.

To illustrate the usefulness of these linkage-specific antibodies, we have used them to examine polyubiquitin editing during signaling by tumor necrosis factor receptor 1 (TNFR1). The kinase adaptor RIP1, for example, is essential for activation of the transcription factor NF-κB following stimulation of TNFR1. RIP1 is recruited to TNFR1 via the adaptor TRADD and must be polyubiquitinated for interaction with NEMO/IKKγ, the regulatory subunit of the inhibitor of κB kinase (IKK), and for recruitment of the kinase TAK1. Activated IKK phosphorylates IκB, which is subsequently ubiquitinated and degraded by the proteasome. NF-κB transcription factors bound to IκB are thereby released and are able to translocate into the nucleus (Hayden and Ghosh, 2008). RIP1 recruited to TNFR1 likely bears K63-linked polyubiquitin, which may be assembled by the E3 TRAF2 (Ea et al., 2006; Lee et al., 2004b; Wertz et al., 2004). A20, which is a negative regulator of TNF-induced NF-κB signaling, functions as a DUB toward RIP1 and, in so doing, disassembles the scaffolding necessary for the recruitment of NEMO and TAK1. Additionally, A20 can function as an E3 ligase and add K48-linked polyubiquitin to RIP1 to target it for proteasomal degradation (Wertz et al., 2004). Using our linkage-specific polyubiquitin antibodies, we have confirmed that RIP1 undergoes polyubiquitin editing and show that chain switching is a more general mechanism for downregulating signaling. We find that IRAK1, a proximal signaling component of the interleukin-1 receptor (IL-1R) and certain Toll-like receptors (TLRs), also undergoes polyubiquitin editing following receptor engagement.

RESULTS

Generation of Polyubiquitin Linkage-Specific Antibodies

We took a phage display approach to engineer antibodies specific for K48- or K63-linked polyubiquitin. A minimal diversity, bivalent Fab antibody fragment phage display library (Fellouse et al., 2007; library D) was panned against ubiquitin chains of either the K63 or K48 linkage (Figure S1A available online). After four rounds of selection, with later rounds including counterselection against monoubiquitin or polyubiquitin of the other linkage, specific binders were identified by an enzyme-linked immunosorbent assay. Twelve clones from each sort were expressed in *E. coli* as soluble Fabs, purified, and tested by surface plasmon resonance (SPR) for binding to K48- and K63-linked polyubiquitin. The highest affinity, most specific clones were then converted to monovalent format and used as templates for second generation libraries with additional sequence diversity engineered into the heavy chain complementarity-determining regions (CDRs) H1, H2, and H3. K48 linkage-selected clones, for instance, had high sequence diversity in CDR H3, so the effect of further diversity in CDR H3 was explored. The K63 linkage-selected clones, by contrast, showed little diversity in CDR H3, so the focus of additional libraries was on optimization of CDRs H1 and H2. Clone Apu2.07 was the highest affinity anti-K48 linkage Fab isolated from a second generation library, with a binding constant of 1.2 nM for K48-linked diubiquitin and no detectable binding to K63-linked diubiquitin (Table 1). Apu2.16 was the highest affinity, most specific anti-K63 linkage Fab with a binding constant of 92 nM for K63-linked diubiquitin and 42 μM for K48-linked diubiquitin. Notably, Apu2.16 and Apu2.07 did not compete for binding to K48-linked diubiquitin (data not shown). Neither Fab demonstrated any detectable binding to monoubiquitin.

Table 1. Binding Constants for Linkage-Specific Anti-Polyubiquitin Fabs

Clone	K48-Linked Diubiquitin K_d (nM)	K63-Linked Diubiquitin K_d (nM)
Apu2.07	1.2	NB
Apu2.16	42000	92
Apu3.A8	NB	8.7
Apu3.A12	NB	6.2
Apu3.B3	NB	6.1

Fab antibody fragments were analyzed by surface plasmon resonance. Due to fast k_{on} and k_{off} rates, only the binding constant (K_d) is reported. NB indicates no detectable binding.

Structural Insights into Fab Recognition of K63-Linked Diubiquitin

To understand the basis of Apu2.16 specificity, the Fab fragment was crystallized in complex with K63-linked diubiquitin. The crystal structure was solved to 2.7 Å (Protein Data Bank [PDB] code 3DVN), and it shows that Apu2.16 recognizes the context of the K63 linkage rather than the linkage itself (Figure 1A). The heart of the recognition motif consists of interactions made by CDR H3, which contacts diubiquitin on either side of the isopeptide linkage. The N-terminal portion of CDR H3 (residues E99, Y100, and Y101) contacts C-terminal residues (72–74) as well as Q40 from the acceptor ubiquitin, while the distal part of H3 (residues R102 and Y103) contacts the 50 s loop of the K63 donor ubiquitin. Specifically, Y103 intercalates into a pocket between the donor ubiquitin 50 s loop and the acceptor G76. The rest of the interface is largely modular with the Apu2.16 light chain CDRs L1 and L2 interacting with the surface of the K63 donor ubiquitin, while the other two heavy chain CDRs contact the acceptor ubiquitin. On the ubiquitin side, the C-terminal residues of the acceptor ubiquitin prior to the isopeptide linkage (especially L73 and R74) are in much more intimate contact with the Fab than the isopeptide linkage itself; these two side chains account for ~25% of the total surface area buried by diubiquitin on complex formation. In contrast, G76 contributes ~1% of ubiquitin surface area, and K63 of the donor ubiquitin does not participate in the interface at all. In addition to extensive Van der Waals interactions, R74 also facilitates electrostatic complementarity to the Fab via a salt bridge to a glutamate side chain (E99) from the proximal part of CDR H3.

Comparison of K63-linked diubiquitin in the above cocrystal to a crystal structure of K63-linked diubiquitin alone (PDB code 2JF5) or to either the crystal (PDB code 1TBE) or solution structures of K48-linked diubiquitin (Cook et al., 1992; Varadan et al., 2002) demonstrates that the Apu2.16 Fab recognizes a specific conformation of diubiquitin that is unique to the K63 linkage (Figure 1B). Moreover, a significant portion of the Fab paratope is derived from CDRs L2 and H2. Because L2 was not

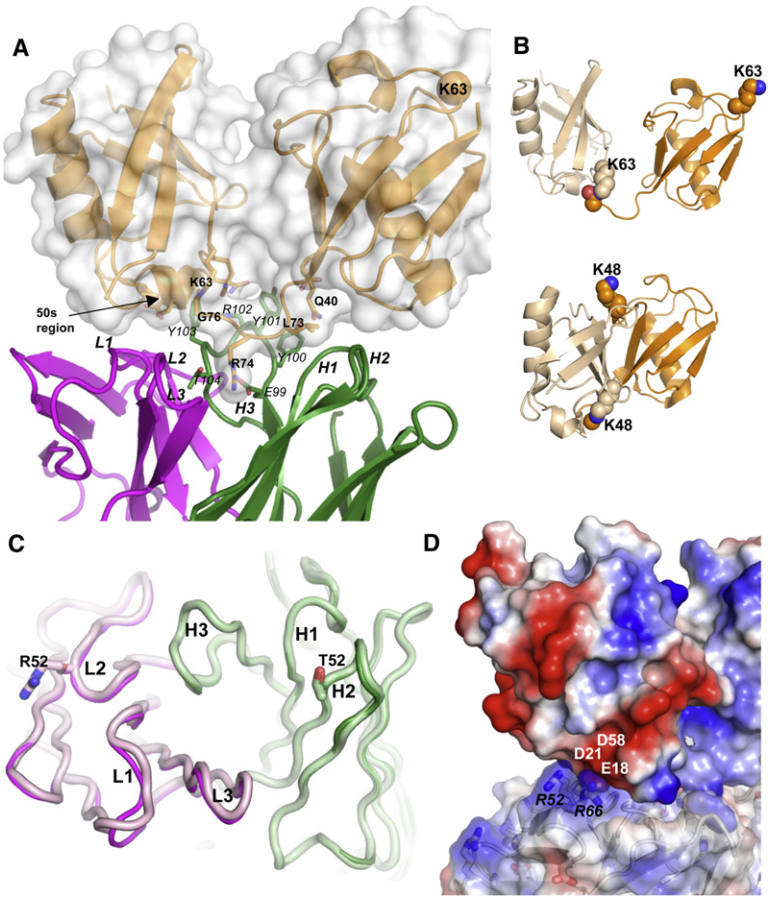

Figure 1. Structural Analysis of Apu2.16 and Apu3.A8 Anti-K63 Linkage Fabs Bound to K63-Linked Diubiquitin

(A) The complex between K63-linked diubiquitin (orange) and the Apu2.16 Fab fragment (heavy chain: green, light chain: magenta). Heavy chain CDR3 (H3) contacts both ubiquitins on either side of the isopeptide linkage. H3 side chains within 4.2 Å of diubiquitin and ubiquitin side chains within 4.2 Å of H3 are shown as sticks. Residues mentioned in the text are in bold for ubiquitin and italics for the Fab. K63 in the acceptor ubiquitin is shown as a sphere.

(B) Comparison of K63- (top) and K48-linked (bottom) diubiquitin. Lysine donor ubiquitins are light orange and acceptor ubiquitins are bright orange. K48-linked diubiquitin forms a more compact shape with the chain extending perpendicular to the ubiquitin dimer, while the K63-linked diubiquitin chain will extend in a more elongated manner.

(C) Superposition of Apu2.16 (colored as in A) and Apu3.A8 (heavy chain: light green, light chain: pink) showing the location of the two changes in L2 (S52R) and H3 (S52T) introduced in the affinity maturation process to create Apu3.A8. The structural differences in L1 in the two Fabs are likely due to crystal packing. L1 (as well as the N terminus) are in a noncanonical conformation likely due to interactions with L3, which has sequence and structural differences relative to the phage library parent sequence (Figure S2).

(D) Charge complementarity between Apu3.A8 (transparent) and diubiquitin (solid). Electrostatic surfaces were calculated with PyMol. Regions of positive potential are blue; regions with negative potential are red. In the Apu3.A8 light chain, R52 (which is introduced in Apu3.A8) and R66 contribute to a positive region that is close to a negatively charged region on the ubiquitin surface, created in part by residues D21, D58, and E18 from the K63 acceptor ubiquitin.

randomized in the first or second generation libraries, Apu2.16 was affinity matured by introducing sequence diversity into paratope positions within CDRs L2 and H2. Three affinity-matured clones, Apu3.A8, Apu3.A12, and Apu3.B3, demonstrated single digit nanomolar binding to K63-linked diubiquitin and no detectable binding to K48-linked diubiquitin (Table 1). Both Apu3.A8 and Apu3.A12 contained a S52R substitution in CDR L2 and a S52T or S52A substitution in CDR H2, respectively (Figure S1B). Apu3.B3 contained four amino acid substitutions.

To understand the structural consequences of the improvements in Apu3.A8, we crystallized the Fab fragment in complex with K63-linked diubiquitin and solved the structure to 2.6 Å resolution (PDB code 3DVG; Figures 1C and S2). Changes in L2 and H2, which improved greatly the specificity and utility of this antibody, had relatively little impact on the structure of the Fab. Excluding differences in the conformation of CDR L1 and the N-terminal strand of the light chain, both of which are attributable to differences in crystal packing, the structures of the two Fabs are virtually identical (rmsd 0.80 Å on 412 C-α atoms). Surprisingly, neither R52 in L2 nor T52 in H2 is in intimate contact with the diubiquitin, and neither residue contributes much to the ubiquitin-binding surface on Apu3.A8. Instead the effect of these two mutations appears to be driven largely by improved electrostatic compatibility between the surface of the K63 donor ubiquitin and the light chain (Figure 1D). In particular, R52 in L2 and R66 in the light chain framework form a positively charged surface patch that complements a negative patch on the surface of the K63 donor ubiquitin.

Western Blotting and Immunoprecipitation using the Polyubiquitin Linkage-Specific Antibodies

The K48 (Apu2.07) and K63 (Apu2.16, Apu3.A8, Apu3.A12, and Apu3.B3) linkage-specific Fabs were converted to full-length human immunoglobulins and tested by western blotting for their ability to recognize polyubiquitin linkages (Figure 2A and data not shown). All five antibodies recognized purified polyubiquitin chains of the appropriate linkage and did not bind to monoubiquitin. The K48 and K63 linkage-specific antibodies (Apu2.07 and Apu3.A8) also detected smears in cell lysates (Figure 2B) derived from human embryonic kidney 293T cells, mouse embryo fibroblasts, insect cells (*Spodoptera frugiperda* Sf9 or *Trichoplusia ni* cells), or yeast (*Saccharomyces cerevisiae* or *Schizosaccharomyces pombe*). Transient transfection of 293T cells with the E3 TRAF6 amplified the K63-linked polyubiquitin signal considerably (Figure 2C), consistent with previous studies characterizing TRAF6 as a K63 ubiquitin ligase (Deng et al., 2000; Wang et al., 2001).

We utilized the observation that overexpressed TRAF6 is itself modified by K63-linked polyubiquitin (Wang et al., 2001) to assess whether the K63 linkage-specific antibody Apu3.A8 would be useful for immunoprecipitation (Figure 2D). When TRAF6-containing lysates were denatured with 1% SDS to

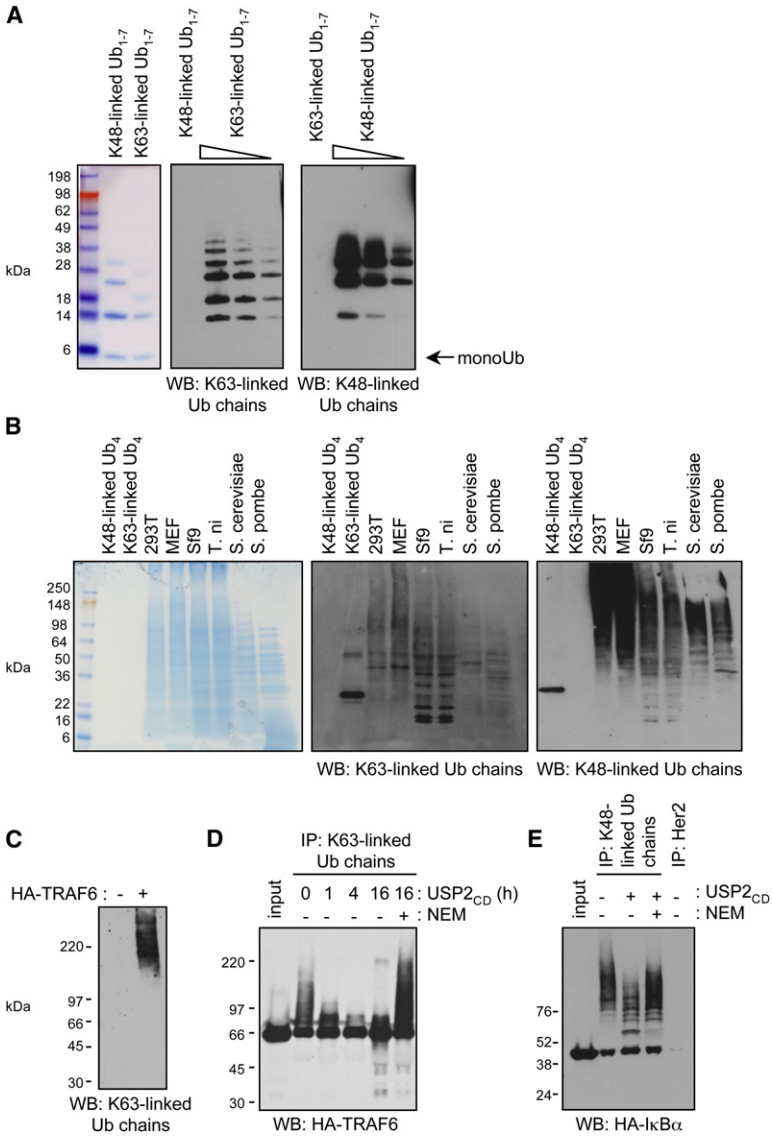

Figure 2. Apu2.07 Anti-K48 Linkage and Apu3.A8 Anti-K63 Linkage Antibodies Western Blot and Immunoprecipitate

(A) Ubiquitin mixtures containing monoubiquitin plus either K48- or K63-linked chains between two and seven ubiquitins in length (1 μg/lane or 1, 0.5, and 0.25 μg/lane where a gradient is indicated) were blotted with Apu2.07 (right panel) or Apu3.A8 (middle panel) IgGs. SimplyBlue SafeStain revealed the composition of the polyubiquitin mixtures (left panel).

(B) Protein extracts from human 293T cells, mouse embryo fibroblasts (MEF), Sf9 and T.ni insect cells, *S. cerevisiae,* and *S. pombe* (50–175 μg extract/lane) were stained with SimplyBlue SafeStain (left panel) or blotted with Apu3.A8 (middle panel) or Apu2.07 (right panel). Control lanes contained K48- or K63-linked tetraubiquitin (0.2 μg).

(C) Overexpression of 3×HA epitope-tagged TRAF6 enhanced the high molecular weight smear detected in 293T cells by Apu3.A8.

(D) Apu3.A8 immunoprecipitated 3×HA-tagged TRAF6 from 293T cells.

(E) Apu2.07 immunoprecipitated 3×HA-tagged IκBα from 293T cells.

dissociate TRAF6 from other ubiquitinated proteins, and immunoprecipitations were performed following dilution of the SDS to as low as 0.05%, no TRAF6 was captured by the K63 linkage-specific antibodies (data not shown). Immunoprecipitation of TRAF6 was successful, however, when TRAF6 lysates were denatured with 6 M urea. Western blot analysis for the 3xHA-epitope tag on TRAF6 revealed a smear of modified protein (Figure 2D, lane 2). Treatment of the immunoprecipitated material with the promiscuous catalytic domain of the DUB USP2 ($USP2_{CD}$) collapsed the higher molecular weight bands, confirming ubiquitination of TRAF6 (Figure 2D, lanes 3–5). Nonspecific proteolytic activity associated with $USP2_{CD}$ did not remove the slower migrating species because inhibition of $USP2_{CD}$ DUB activity with the cysteine protease inhibitor N-ethylmaleimide (NEM) prevented collapse of the smear (Figure 2D, lane 6). A portion of the TRAF6 immunoprecipitated by the K63 linkage-specific antibody appeared, by its migration, to be unmodified TRAF6. We speculate that a cellular DUB was not inactivated fully upon lysis and that this DUB generated the faster-migrating species of TRAF6 during the immunoprecipitation. The ability of the K48 linkage-specific antibody to immunoprecipitate K48-linked polyubiquitinated proteins was determined using overexpressed 3xHA-tagged IκBα. A smear of IκBα was immunoprecipitated by the K48 linkage-specific antibody, which was converted to a faster migrating smear by $USP2_{CD}$ in a NEM-sensitive manner (Figure 2E). An isotype control antibody recognizing human HER2 failed to immunoprecipitate either IκBα or TRAF6 (Figure 2E and data not shown).

Confirmation of Antibody Linkage Specificity by Mass Spectrometry

Having established that the K48 and K63 linkage-specific antibodies could immunoprecipitate polyubiquitinated proteins, we sought to confirm their linkage specificity in this application using mass spectrometry. Polyubiquitinated proteins were immunoprecipitated from human BJAB cells, resolved by SDS-PAGE, subjected to in-gel trypsin digestion, and then analyzed using a variation of the ubiquitin-AQUA method (Kirkpatrick et al., 2006). Briefly, trypsin digests were supplemented with isotope-labeled internal standard peptides representing each polyubiquitin chain linkage and unbranched ubiquitin, and then the standards plus their corresponding native analytes were detected in high-resolution precursor ion scans using narrow range-extracted ion chromatograms. The abundance of each polyubiquitin chain linkage and the total amount of ubiquitin in the BJAB immunoprecipitates were quantified by comparing the signal from each digested peptide relative to its corresponding internal standard. The anti-K48 linkage, anti-K63 linkage (Apu3.A8), and isotype control antibodies immunoprecipitated 49.1 pmol, 2.2 pmol, and 0.2 pmol of total ubiquitin, respectively (Figure 3A). This result was in keeping with the observation

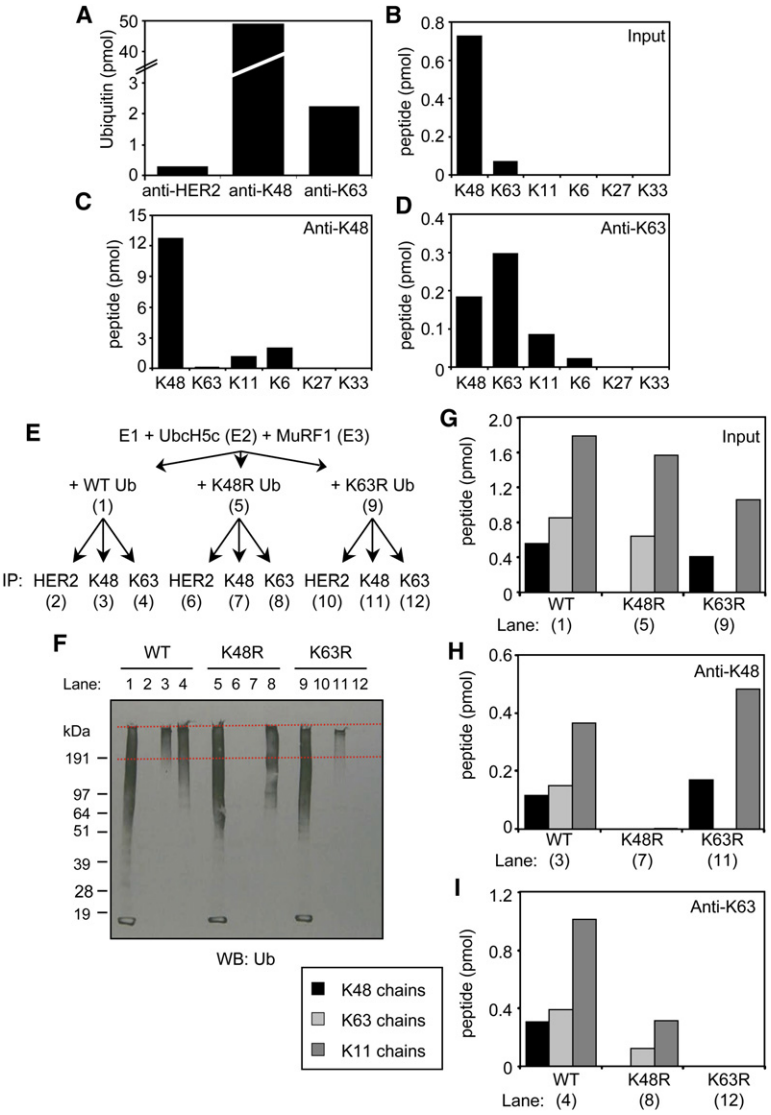

Figure 3. Mass Spectrometry Confirms the Linkage Specificity of Apu2.07 and Apu3.A8 in Immunoprecipitations

(A–D) BJAB cell lysates were immunoprecipitated with Apu2.07, Apu3.A8, or an isotype control antibody recognizing HER2. Mass spectrometry was used to determine the total amount of ubiquitin immunoprecipitated (A) as well as the polyubiquitin linkages in the lysate (B) and immunoprecipitates (C and D).

(E) MuRF1 autoubiquitination reactions performed in vitro with WT, K48R, or K63R ubiquitin were immunoprecipitated with Apu2.07, Apu3.A8, or isotype control. Numbers in parentheses indicate the relevant lanes and columns in (F)–(I).

(F) Autoubiquitination reactions and immunoprecipitations depicted in (E) were western blotted with a pan-ubiquitin antibody. The hatched red lines indicate the portion of the gel that was cut out and subjected to analysis by mass spectrometry.

(G–I) Mass spectrometry was used to determine the polyubiquitin linkages in the autoubiquitination reactions and immunoprecipitations depicted in (E).

that K48-linked polyubiquitin was more abundant than K63-linked polyubiquitin in the input lysate used for the immunoprecipitations (Figure 3B). Direct examination of the polyubiquitin linkages immunoprecipitated by the anti-K48 linkage antibody revealed 12.7 pmol of K48 –GG signature peptide and measurable amounts of the signature peptides for other linkages: 0.1 pmol K63, 1.1 pmol K11, and 2.0 pmol K6 (Figure 3C). Similarly, polyubiquitin immunoprecipitated by the anti-K63 linkage antibody did not produce exclusively the K63 –GG signature peptide; 0.3 pmol K63, 0.18 pmol K48, 0.08 pmol K11, and 0.06 pmol K6 were detected (Figure 3D). Given the strong binding preferences seen for the antibodies by SPR (Table 1), these mass spectrometry results suggest that a significant fraction of ubiquitin-modified cellular substrates (or complexes that resist dissociation in 6 M urea) exhibit heterogeneous polyubiquitin chain linkages.

To confirm that the mixed linkages immunoprecipitated from BJAB cell lysates derived from substrates bearing heterogeneous polyubiquitin chains, as opposed to nonspecific binding, we tested whether the target linkage was necessary for immunoprecipitation of the other linkage types. Mixed linkage polyubiquitin chains with either the K48 or K63 linkage absent were generated in vitro using the E3 MuRF1 and the E2 UbcH5c (Kim et al., 2007). The K48 or K63 linkage was excluded from the MuRF1 autoubiquitination reactions using mutant ubiquitin that had either K48 or K63 mutated to arginine (Figure 3E). By western blotting with a pan ubiquitin antibody, MuRF1 autoubiquitination reactions produced high molecular weight smears irrespective of whether we used wild-type (WT), K48R, or K63R ubiquitin (Figure 3F, lanes 1, 5, and 9). Ubiquitin-AQUA analysis of the reaction with WT ubiquitin revealed three main linkages: K48, K63, and K11 (Figure 3G, lane 1). As expected, reactions performed with K48R ubiquitin lacked K48-linked chains (Figure 3G, lane 5) and those performed with K63R ubiquitin lacked K63-linked chains (Figure 3G, lane 9). Both the anti-K48 and anti-K63 linkage antibodies immunoprecipitated polyubiquitinated species when MuRF1 was modified with WT ubiquitin (Figure 3F, lanes 3 and 4), but each antibody failed to do so if their target linkage was absent (Figure 3F, lanes 7 and 12). An isotype control antibody did not immunoprecipitate ubiquitinated MuRF1 from any of the reactions (Figure 3F, lanes 2, 6, and 10). Ubiquitin-AQUA analysis of the immunoprecipitated species from the WT ubiquitin reaction demonstrated the presence of K48-, K63-, and K11-linked chains regardless of the antibody used for enrichment (Figure 3H, lane 3 and Figure 3I, lane 4). As predicted by western blotting (Figure 3F, lanes 7 and 12), K11-linked chains were immunoprecipitated by both the anti-K48 and anti-K63 linkage antibodies only if their target linkage was also present (Figures 3H and 3I). These results demonstrate that the anti-K48 and anti-K63 linkage antibodies retain their fidelity in the context of immunoprecipitation. Further, they

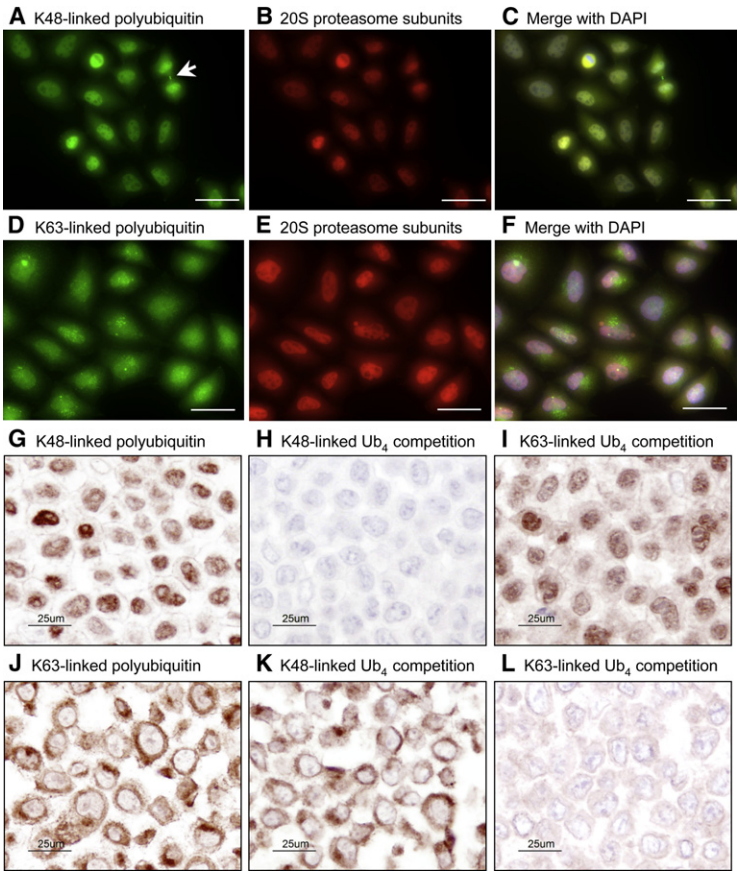

Figure 4. Immunofluorescent and Immunohistochemical Staining of K48- and K63-Linked Polyubiquitin

(A–F) HeLa cells were stained with Apu2.07 (A), Apu3.A8 (D), and a polyclonal antibody recognizing 20S proteasome subunits (B and E). The arrow indicates mid-body staining. In the merged images (C and F), yellow staining indicates potential colocalization and blue staining corresponds to DAPI-labeled nuclei. Bars, 50 μm.

(G–L) HeLa cells harvested 1 hr after UV irradiation (50 J/m^2) were stained with Apu2.07 (G–I) or Apu3.A8 (J–L). Antibody specificity was assessed by preincubating the antibodies with either K48- (H and K) or K63-linked tetraubiquitin (I and L).

indicate that alternative linkages immunoprecipitated from cells by the K48 and K63 linkage-specific antibodies must stem from individual substrates (or complexes not dissociated by 6 M urea) bearing both the target linkage and other linkage types. Whether individual chains contain mixed linkages or whether substrates carry polyubiquitin chains of different linkages on separate lysines remains to be determined.

Localization of K48- and K63-linked Polyubiquitin within Cells

We used the linkage-specific polyubiquitin antibodies to determine the distribution of K48- and K63-linked polyubiquitin within cells by indirect immunofluorescence microscopy (Figures 4A and 4D). Apu2.07 anti-K48 linkage antibody stained both the nucleus and cytoplasm of HeLa cells, but what appeared to be nucleoli within the nucleus were labeled less intensely (Figure 4A). This pattern of staining coincided almost completely with proteasomes labeled with a polyclonal antibody recognizing the core 20S subunits (Figures 4B and 4C), which is consistent with the notion that K48-linked polyubiquitin generally targets proteins for proteasomal degradation. Interestingly, K48-linked polyubiquitin, but not proteasomes, was detected at the midbody during mitosis. Apu3.A8 anti-K63 linkage antibody had a very different staining pattern, labeling cytoplasmic speckles that varied both in number and size between individual cells (Figure 4D). We did not detect colocalization of K63-linked polyubiquitin with proteasomes in these speckles (Figures 4E and 4F). Nor did the K63-linked polyubiquitin speckles colocalize with Golgi complex and lysosomal markers (Figure S3). In control experiments, staining by the linkage-specific antibodies could be competed by synthesized polyubiquitin only if the chains contained the target linkage (data not shown). These results indicate that K48- and K63-linked polyubiquitin can occur in distinct subcellular regions.

We also tested whether the linkage-specific antibodies would be useful for immunohistochemistry and found that formalin-fixed, paraffin-embedded sections of HeLa cells also were stained effectively by the Apu2.07 anti-K48 and Apu3.A8 anti-K63 linkage antibodies (Figures 4G and 4J). Staining was competed by tetraubiquitin containing the target linkage but not by tetraubiquitin containing an alternative linkage (Figures 4H, 4I, 4K, and 4L).

RIP1 Undergoes Polyubiquitin Chain Editing

The utility of the K48 and K63 linkage-specific antibodies in unveiling the type of ubiquitination on a specific target protein was assessed with endogenous RIP1 in HeLa S3 cells treated with TNF (Figure 5). It has been shown that RIP1 recruited to TNFR1 is polyubiquitinated (Ea et al., 2006; Legler et al., 2003; Wertz et al., 2004) and, based on in vitro and overexpression studies, K63-linked polyubiquitin on RIP1 supports downstream signaling events resulting in NF-κB activation (Ea et al., 2006). The K63-linked polyubiquitin eventually is replaced with K48-linked chains by A20, which has dual function as a DUB and K48-promoting E3 (Wertz et al., 2004). The A20 gene is a transcriptional target of NF-κB and thus forms part of a negative feedback loop to terminate NF-κB signaling (Hayden and Ghosh, 2008). Consistent with previous results (Ea et al., 2006; Legler et al., 2003; Wertz et al., 2004), a smear of RIP1 was associated with TNFR1 within 5 min of TNF addition (Figure 5B), and this coincided with degradation of IκBα (Figure 5A), which served as our readout for activation of the NF-κB pathway. Modified RIP1 was less abundant at later time points (Figure 5B), which is consistent with a previous study showing that RIP1 polyubiquitinated in response to TNF is degraded by the proteasome (Legler et al., 2003). Next we immunoprecipitated TNFR1-containing complexes at different times after treatment with TNF, dissociated the receptor complexes

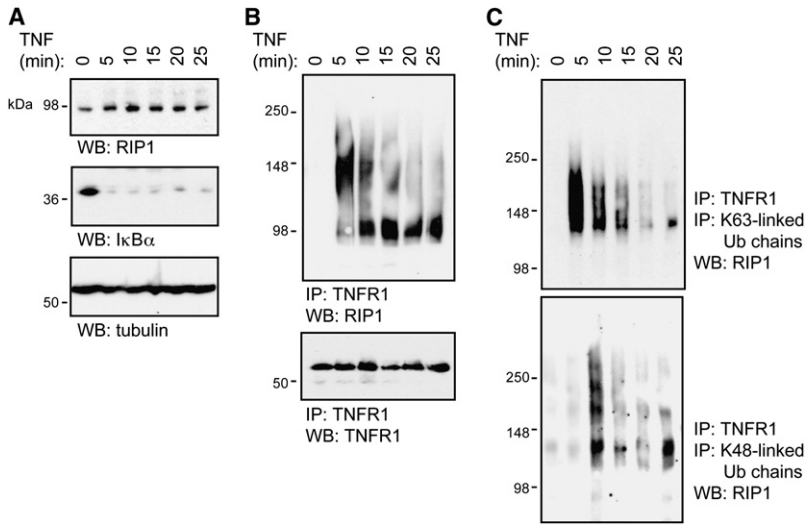

Figure 5. Linkage-Specific Polyubiquitin Antibodies Reveal Chain Editing of RIP1 in TNF-Treated Cells

HeLa cells pretreated with 21 μM MG-132 for 10 min were stimulated with 100 ng/ml TNF. Western blots show total RIP1, IκBα, and tubulin levels (A), immunoprecipitated TNFR1 and associated RIP1 (B), and RIP1 that is associated with TNFR1 and is polyubiquitinated with K63- (C, upper panel) or K48-linked chains (C, lower panel). Complete proteasome inhibition in cells by MG-132 pretreatment is not apparent until approximately 45 min post-addition (Figure S4), so IκBα and RIP1 modified by K48-linked polyubiquitin can be degraded at the times shown.

in 6 M urea, and then immunoprecipitated with either the K48 or K63 linkage-specific polyubiquitin antibodies before blotting for RIP1. This experiment revealed that TNFR1-associated RIP1 was modified almost entirely by K63-linked chains at 5 min (Figure 5C). The intensity of the K63-linked polyubiquitin signal on RIP1 was decreased at 10 min and K48-linked polyubiquitin was detected, the latter also diminishing at later times presumably as a result of proteasomal degradation of RIP1. These results confirm that TNFR1-associated RIP1 undergoes polyubiquitin editing during TNFR1 signaling.

IRAK1 Undergoes Polyubiquitin Chain Editing

Given that RIP1 is modified sequentially by K63- and then K48-linked polyubiquitin, the latter being conferred by E3 A20, and that A20 also is a negative regulator of signaling by certain TLRs (Boone et al., 2004), we investigated whether other kinase adaptors recruited to TLRs and the IL-1R might be regulated in a similar fashion. IRAK1 appeared a good candidate for undergoing polyubiquitin editing because posttranslationally modified IRAK is recruited rapidly to activated receptor complexes and subsequently is degraded (Yamin and Miller, 1997). We treated 293 cells stably expressing the IL-1R with IL-1β, and consistent with the work of Yamin and Miller (1997), western blotting revealed a smear of modified IRAK1 within 2 min (Figure 6A). The slower migrating forms of IRAK1 were more abundant at 10 min and could be converted to the unmodified form of IRAK1 by $USP2_{CD}$ in a NEM-sensitive manner. These results suggest that the higher molecular weight forms of IRAK1 are due to ubiquitination. The appearance of ubiquitinated IRAK1 coincided with activation of downstream NF-κB signaling as evidenced by IκBα degradation (Figure 6B). At different times after treatment with IL-1β, we also prepared cell lysates in 6 M urea and then immunoprecipitated with the linkage-specific antibodies prior to western blotting for IRAK1 (Figure 6C). IRAK1 modified with K63-linked polyubiquitin was detected at 5 min and was maximal by 30–60 min, which mirrored the kinetics of appearance of the high molecular weight IRAK1 smear (compare the upper panels of Figures 6B and 6C). The amount of K48-linked polyubiquitin evident on IRAK1 peaked at 90–150 min, which is when the intensity of the total IRAK1 signal began to subside. When cells treated with IL-1β were not pretreated with proteasome inhibitor MG-132, this degradation of ubiquitinated IRAK1 was accelerated (Figure S4), consistent with the K48-linked polyubiquitin targeting IRAK1 for the proteasome. Thus polyubiquitin editing of IRAK1 in cells treated with IL-1β resembles that of RIP1 in cells treated with TNF, and this process of chain editing may represent a general mechanism of terminating downstream signaling events.

DISCUSSION

Our rationale for developing antibodies with the ability to discriminate between polyubiquitin chain linkages is that they represent the best tools for addressing whether chain linkage is a major determining factor in the fate of polyubiquitinated proteins. The first indication that different chain linkages might have unique functions came from the study of yeast mutants in which either K48 or K63 of ubiquitin was mutated to arginine; K63-linked polyubiquitin was implicated in DNA repair (Spence et al., 1995), whereas K48-linked polyubiquitin was important for protein degradation and for progression through the cell cycle (Finley et al., 1994). Assessment of polyubiquitin chain linkage on modified mammalian proteins commonly involves immunoprecipitation of the protein from cells overexpressing epitope-tagged ubiquitin mutants and/or in vitro ubiquitination assays with the same ubiquitin mutants (for examples, see Ea et al., 2006; Wang et al., 2001; Wertz et al., 2004). The potential pitfalls of using ubiquitin mutants are (1) the E2 and/or E3 might be sensitive to lysine mutations at nonlinkage sites, (2) other lysines might be used when the preferred lysine is absent, and (3) incomplete penetration of the mutant ubiquitin into the total pool of cellular ubiquitin may limit its ability to interfere dominantly with specific linkage-mediated events. The impact of epitope tags on ubiquitin chain assembly also is unclear. Diagnostic antibodies that recognize specific polyubiquitin chain linkages and can be used for immunoprecipitation and western blotting therefore provide the quickest, simplest means of determining polyubiquitin chain linkage.

The use of a minimalist diversity phage display library in combination with powerful in vitro selection methods was critical to our success in generating high-affinity, linkage-specific

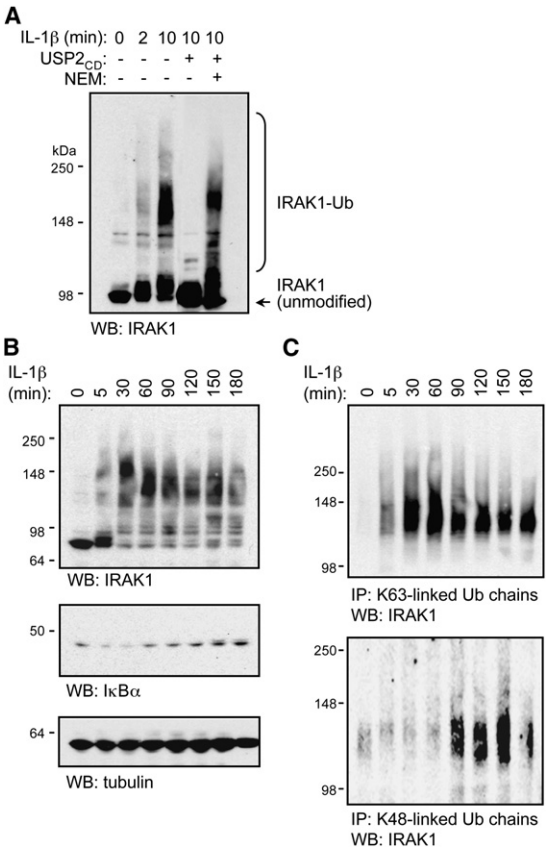

Figure 6. Linkage-Specific Polyubiquitin Antibodies Reveal Chain Editing of IRAK1 in IL-1β-Treated Cells

293 cells stably expressing the IL-1 receptor were pretreated with 25 μM MG-132 for 10 min and then stimulated with 10 ng/ml IL-1β. Western blots show total IRAK1, IκBα, and tubulin levels (A and B) and IRAK1 that is modified by K63- (C, upper panel) or K48-linked polyubiquitin (C, lower panel).

antibodies to polyubiquitin. Indeed, exhaustive efforts to generate polyubiquitin linkage-specific antibodies by traditional immunization strategies proved futile, probably reflecting the inability of the naturally occurring antibody repertoire to recognize these highly conserved epitopes. The minimalist library was key because we did not enrich for specific binders using a synthetic library with CDRs based on natural diversity (Lee et al., 2004a). CDR H3 typically makes the largest contribution to antigen recognition, so the minimalist library provides complex diversity in CDR H3 to allow selection for specific interactions, while binary diversity (Ser or Tyr) in the other CDRs minimizes steric hindrance and enables adaptation to varied surfaces. Of note, however, initial binders from this library are often low affinity and require affinity optimization. Refinement of the anti-K48 polyubiquitin linkage antibody was accomplished readily by engineering additional diversity into CDR H3 and repeating the selection process. The resulting anti-K48 linkage Fab, Apu2.07, was of high affinity and specificity. By contrast, the anti-K63 linkage Fab, Apu2.16, had additional diversity in CDRs H1 and H2 but it required even further affinity maturation. The structure of Apu2.16 in complex with K63-linked diubiquitin (Figure 1) guided construction of third generation libraries. By focusing on the important contacts between K63-linked diubiquitin and CDRs L2 and H2, we obtained clones that were of sufficient affinity and specificity for characterization of K63-linked polyubiquitination in cells.

We focused on the generation of K48 and K63 linkage-specific polyubiquitin antibodies because these linkages are the best studied to date (Hershko and Ciechanover, 1998). Mass spectrometry, in combination with enrichment strategies to capture ubiquitinated proteins in yeast (Peng et al., 2003) or in mouse brain (Bennett et al., 2007), has shown that K48 linkages are dominant, while K63 and K11 linkages are the next most abundant. K33, K27, and K6 linkages have been detected in yeast but appear to be present at much lower levels (Peng et al., 2003). K48 and K63 linkages dominated our BJAB cell lysates (Figure 3B), but K6 and K11 linkages were detected following enrichment with either the K48 or K63 linkage-specific antibodies (Figures 3C and 3D). These alternative linkages did not represent nonspecific binding of the polyubiquitin antibodies because they could only be immunoprecipitated from in vitro autoubiquitination reactions when the target linkage was present (Figures 3H and 3I). These data could indicate that a significant fraction of polyubiquitinated substrates within cells bear heterogeneous chain linkages. Unfortunately, the methodologies used do not discern whether substrates carry polyubiquitin chains of mixed linkages or several different chains each of a uniform linkage. It also is possible that the heterogeneous polyubiquitin chain linkages stem from coprecipitating proteins that resist dissociation in 6 M urea.

Polyubiquitin modifications are well described in the signaling pathways triggered by cytokines TNF and IL-1β, so we used these systems to demonstrate the power of the linkage-specific antibodies for interrogating ubiquitin chain editing during signal transduction in vivo (Figures 5 and 6). Previously, we showed by coexpressing mutant ubiquitins with all but one lysine mutated to arginine that RIP1 acquires K63-linked polyubiquitin in the presence of E3 TRAF2 (Wertz et al., 2004). Indeed, TNF-induced RIP1 polyubiquitination is defective in TRAF2-deficient MEFs (Lee et al., 2004b). The K63-linked polyubiquitin on overexpressed RIP1 can be replaced with K48-linked polyubiquitin by A20 (Wertz et al., 2004). We now demonstrate directly using our linkage-specific antibodies that endogenous RIP1 recruited to TNFR1 is modified transiently by K63-linked polyubiquitin as NF-κB is activated and then is modified by K48-linked polyubiquitin (Figures 5C and S5A). The latter modification coincides with degradation of TNFR1-associated RIP1 (Figure 5B) and termination of NF-κB signaling.

We also show that endogenous IRAK1 exhibits a similar pattern of polyubiquitination in cells treated with IL-1β (Figures 6 and S5B). IRAK1 is recruited to the IL-1R (and certain TLRs), where it is phosphorylated and subsequently degraded (Yamin and Miller, 1997). TRAF6 is reported to assemble K63-linked polyubiquitin on IRAK1 (Conze et al., 2008) although Pellino proteins have been implicated in IRAK1 ubiquitination also (Ordureau et al., 2008; Xiao et al., 2008). This polyubiquitination has been suggested to mediate recruitment of NEMO for NF-κB activation (Conze et al., 2008; Windheim et al., 2008), although one study of IRAK1-deficient cells indicated that IRAK1 was dispensable for

IL-1β-induced NF-κB activation at higher doses of IL-1β (Kanakaraj et al., 1998), perhaps due to functional redundancy with IRAK2. Given that IRAK1 and the ubiquitin-dependent kinase TAK1 are both essential for IL-1β-induced activation of MAP kinases p38 and JNK (Kanakaraj et al., 1998; Thomas et al., 1999; Sato et al., 2005), K63-linked polyubiquitination of IRAK1 might also contribute to activation of TAK1. Phosphorylation and polyubiquitination of IRAK1 occur normally in TAK1-deficient cells treated with IL-1β, consistent with TAK1 acting downstream of IRAK1 (Sato et al., 2005).

IRAK1 activated by the IL-1R eventually is degraded (Figure 6 and Yamin and Miller, 1997). The reduction in IRAK1 correlates with modification of IRAK1 by K48-linked polyubiquitin so these chains likely target IRAK1 for proteasomal degradation. Indeed, we find that the proteasome inhibitor MG-132 can abrogate IRAK1 degradation (Figure S4). It remains to be determined whether a dual function E3/DUB such as A20 is responsible for the ubiquitin chain switching on IRAK1. Because both RIP1 and IRAK1 undergo chain editing as a means of downregulating cytokine signaling, it will be interesting to determine whether other kinases are regulated in this manner.

EXPERIMENTAL PROCEDURES

Phage Display

Phage display libraries were generated and sorted as described (Sidhu et al., 2000). SPR was done using a BIACORE A100 or 3000. K63- or K48-linked diubiquitin (~50 resonance units; Boston Biochem) were immobilized on a CM5 chip using an amine coupling protocol. For reference subtraction, a spot was activated and ethanolamine blocked without immobilizing protein. Serial dilutions (31.25–500 nM) of Fabs were injected (60 μl total at 30 μl/min). The chip was regenerated with 15 μl of 10 mM HCl after 10 min. Kinetic and binding constants were calculated by nonlinear regression analysis. Fab variable domains were cloned into pRK vectors encoding the heavy chain of human IgG1 and a human kappa light chain. IgGs were expressed transiently in 293 or CHO cells and purified on protein A- or protein G-sepharose.

Crystallography

Fab fragments expressed in *E. coli* were purified with protein G-sepharose (0.58% acetic acid elution) and then a SP HiTrap column (GE) with 20 mM MES pH 5.5 and a NaCl gradient. A S-200 column (GE) in 20 mM Tris-HCl (pH 7.3), 150 mM NaCl also was used for Apu3.A8. K63-linked diubiquitin was produced according to Pickart and Raasi (2005) and purified with a MonoS column in a NaCl gradient and 20 mM MES (pH 5.5). Fab-diubiquitin complexes were purified on a Superdex 75 column in 20 mM Tris-HCl (pH 7.3), 150 mM NaCl. Apu2.16 crystals grew in 2 weeks at 18°C in sitting drops from a 1:1 mixture of protein (12.7 mg/ml in 10 mM Tris-HCl pH 8.0, 75 mM NaCl) and well solution (0.2 M NaCl, 0.1 M Tris pH 8.2, 0.1 M citrate). For cryoprotection, well solution contained 18% glucose. Apu3.A8 crystals grew after 2 weeks at 18°C in sitting drops from 1:1 mixtures of protein (17 mg/ml in 20 mM Tris-HCl pH 7.3, 150 mM NaCl) and well solution (0.1 M Tris-HCl pH 8.0, 1.6 M $LiSO_4$). For cryoprotection, well solution contained 30% glycerol. Data were collected at SSRL beamlines 9-2 (Apu2.16 complex) and 7-1 (Apu3.A8) (Table S1) and were processed with HKL. Structures were solved by molecular replacement using PHASER (CCP4) and refined with REFMAC5 (CCP4). For the Apu2.16 complex, the humanized 4D5 Fab (PDB code 1FVE) and ubiquitin (PDB code 1UBQ) were used as search models. The Apu3.A8 complex was solved using the refined Apu2.16 complex as a search model. All figures were made with PyMol (http://www.pymol.org).

Mass Spectrometry

Burkitt lymphoma BJAB cells (>10^9) were washed in PBS and lysed for 30 min at room temperature in lysis buffer (20 mM Tris-HCl pH 7.5, 135 mM NaCl, 1.5 mM $MgCl_2$, 1 mM EGTA, 1% Triton X-100, 10% glycerol) containing 6 M urea, 2 mM N-ethylmaleimide (NEM), and protease inhibitors (Roche). The soluble lysate was diluted to 4 M urea with lysis buffer (supplemented with protease inhibitors, 2 mM NEM, and 1 mM DTT) and precleared with protein A-sepharose for 1 hr. The lysate was divided into three samples, which received either 30 ug of Apu3.A8 IgG, Apu2.07 IgG, or isotype control antibody Herceptin. Samples were mixed for 2 hr, then centrifuged to remove precipitated material. Further antibody (10 ug) plus protein A-sepharose was added and the samples were mixed overnight. The sepharose beads were washed extensively in lysis buffer and once in PBS before elution in reducing SDS sample buffer. Proteins were alkylated with iodoacetamide and resolved by SDS-PAGE. Excluding the 25 and 55 kDa regions, the rest of each gel lane was washed in 25 mM NH_4HCO_3 in 50:50 acetonitrile:water and dehydrated. Gel pieces were rehydrated in 25 mM NH_4HCO_3 containing trypsin (Promega), incubated overnight at 37°C, and then extracted once in 5% acetic acid and twice in 100% acetonitrile. The peptide digests were spiked with AQUA peptide standards (1 pmol) and separated on a NanoAcquity UPLC system (Waters) with a precolumn (5 μm Symmetry C18, 180 × 20 mm) and an analytical column (1.7 μm BEH-130 C18 column 100 × 100 mm, Waters), using a 70 min gradient from 2% to 90% solvent B (solvent A is water + 0.1% formic acid; solvent B is 100% acetonitrile + 0.1% formic acid) and a total analysis time of 90 min. Peptides were eluted directly into a nanospray ionization source with a spray voltage of 2 kV and analyzed using an LTQ XL-Orbitrap mass spectrometer (ThermoFisher). Precursor ions were analyzed in the FTMS at 60,000 resolution. Quantitation was performed by comparing peak areas for the heavy and light versions of each peptide, extracting the ion chromatograms at 10 ppm mass accuracy to 4 decimal places.

MuRF1 autoubiquitination reactions were performed according to the manufacturer (Boston Biochem). For immunoprecipitations, samples were diluted 100-fold in lysis buffer containing 4 M urea, precleared with protein A-sepharose, and then incubated overnight with antibody (20 ug) and protein A-sepharose. Total ubiquitin was blotted with P4D1 antibody (Santa Cruz Biotechnology). For mass spectrometry, samples were resolved on an Agilent 1100 LC module with a 15 min gradient from 5% to 30% Solvent B and a total analysis time of 30 min. Ion chromatograms were created by extracting a window ± 15 ppm from the expected m/z.

Immunoprecipitation, Western Blotting, and Deubiquitination

293T cells were transfected with 3×HA-tagged versions of human IκBα or TRAF6 using Lipofectamine 2000 (Invitrogen). Cells were lysed 36 hr later in lysis buffer containing 6 M urea, a complete protease inhibitor cocktail, and 2 mM NEM. Immunoprecipitations were as described above except that samples were diluted with lysis buffer to 0.3 M urea and were performed at 4°C. Beads were washed sequentially in lysis buffer, PBS, and DUB reaction buffer (40 mM sodium phosphate pH 8, 150 mM NaCl, 2 mM DTT, 10% glycerol). Where indicated, beads were incubated at 25°C with $USP2_{CD}$ (Boston Biochem) ± 5 mM NEM. Sf9 and T.ni cells were harvested in lysis buffer containing protease inhibitors. 293T and C57BL/6 mouse embryo fibroblast lysates also contained 1 mM DTT, 2 mM NEM, and a PhosSTOP cocktail (Roche). *S. cerevisiae* YRG-2 and *S. pombe* SP-Q01 cells (Stratagene) grown in YPD and YES medium, respectively, were extracted in Y-PER (Pierce) supplemented with 5 mM DTT, 2 mM NEM, and 25 μM MG-132 (Calbiochem). Polyubiquitin blotted with Apu2.07 and Apu3.A8 was revealed with peroxidase-conjugated goat anti-human IgG (Cappel).

HeLa S3 cells were treated with 21 μM MG-132 for 10 min prior to addition of 100 ng/ml TNF (Genentech). Cells were lysed at 4°C in TNFR1 immunoprecipitation buffer (20 mM Tris-HCl pH 7.5, 150 mM NaCl, 1% Triton X-100, and 1 mM EDTA) containing protease and phosphatase inhibitors, 25 μM MG-132, 10 mM NEM, and 50 mM NaF. For immunoprecipitations, the soluble lysate was precleared with protein A-sepharose for 1 hr and then incubated with anti-TNFR1 antibody (Genentech) plus protein A-sepharose at 4°C for 5 hr. Beads were washed twice with TNFR1 immunoprecipitation buffer, twice with TNFR1 immunoprecipitation buffer containing 1 M NaCl, and twice with TNFR1 immunoprecipitation buffer. Proteins were eluted in lysis buffer containing 6 M urea. For serial immunoprecipitations, samples were diluted 25-fold with lysis buffer containing protease inhibitors, 10 mM NEM, and 0.5 mM DTT, precleared with protein A-sepharose plus Herceptin, and then

incubated with either Apu2.07 or a 1:1 mix of Apu3.A8 and Apu3.B3 precoupled to protein A-sepharose for 2 hr at 4°C. Antibodies used for western blotting recognized RIP1 (BD Biosciences), β-tubulin (ICN Biomedicals), and IκBα (Cell Signaling Technology).

293 cells stably expressing IL-1R and IL1R-AcP were treated with 25 μM MG-132 for 10 min prior to addition of 10 ng/ml IL-1β. Cells were lysed in IRAK immunoprecipitation buffer (20 mM HEPES pH 7.6, 150 mM NaCl, 1.5 mM $MgCl_2$, 2 mM EGTA, 10 mM NaF, 2 mM DTT, and 0.5% Triton X-100) containing 6 M urea. Soluble lysates were diluted 20-fold and incubated with either Apu2.07 or a 1:1 mix of Apu3.A8 and Apu3.B3 as described above for RIP1.

Immunofluorescence Staining

HeLa cells were fixed with 4% paraformaldehyde in PBS at room temperature for 20 min, rinsed twice with PBS, and permeabilized with PBS containing 0.1% Triton X-100 for 5 min. Nonspecific binding sites were blocked with Earle's balanced salt solution containing 10% goat serum, 0.1% Triton X-100, and 0.1% saponin for 1 hr, then cells were labeled overnight at 4°C with 1 μg/ml Apu2.07, 1 μg/ml Apu3.A8, or 5 μg/ml PW8155 anti-proteasome (Biomol International). Cells were washed three times with PBS containing 0.1% Triton X-100 and incubated for 15 min with four drops of Image-IT Fx signal enhancer (Invitrogen). After three washes with PBS containing 0.1% Triton X-100, the cells were stained for 1 hr with Cy2-conjugated anti-human and Texas Red-conjugated anti-rabbit antibodies (Jackson ImmunoResearch). Cells were washed three times with PBS containing 0.1% Triton X-100, rinsed twice with water, and mounted with ProLong Gold containing DAPI (Invitrogen). Images obtained with an Axioplan 2 light microscope (Carl Zeiss MicroImaging) were recorded with a $CoolSNAP_{HQ}$ CCD camera (Photometrics).

Immunohistochemical Staining

Formalin-fixed, paraffin-embedded 3 μm sections were deparaffinized in xylenes and rehydrated through a graded alcohol series. Antigen retrieval was performed in Trilogy (Cell Marque) for Apu2.07 and Target high pH Retrieval Solution (DAKO) for Apu3.A8. Endogenous peroxidase activity was blocked with KPL blocking solution (Kirkegaard and Perry Laboratories), which was followed by an avidin/biotin block (Vector Labs), and then nonspecific binding sites were blocked with PBS containing 10% goat serum and 3% BSA. Staining was for 1 hr with 1 μg/ml Apu2.07 or 5 μg/ml Apu3.A8. Where indicated, antibody was preincubated for 1 hr with a 10-fold excess of K48- or K63-linked tetraubiquitin (Boston Biochem). Immunostaining was completed with biotinylated goat anti-human IgG (Vector Labs), ABC-HRP Elite reagent (Vector Labs), and metal enhanced DAB substrate (Pierce). Sections were counterstained with Myer's Hematoxylin (Rowley Biochemical Institute).

ACCESSION NUMBERS

The Apu2.16-K63-linked diubiquitin and Apu3.A8-K63-linked diubiquitin structures were deposited in the Protein Data Bank with codes 3DVN and 3DVG, respectively.

SUPPLEMENTAL DATA

Supplemental Data include one table and five figures and can be found with this article online at http://www.cell.com/cgi/content/full/134/4/668/DC1/.

ACKNOWLEDGMENTS

We thank Ahn Pham for assistance with the second generation libraries and Allison Bruce for helping with figure preparation. All authors were employees and shareholders of Genentech, Inc.

Received: May 6, 2008
Revised: June 26, 2008
Accepted: July 29, 2008
Published: August 21, 2008

REFERENCES

Bennett, E.J., Shaler, T.A., Woodman, B., Ryu, K.Y., Zaitseva, T.S., Becker, C.H., Bates, G.P., Schulman, H., and Kopito, R.R. (2007). Global changes to the ubiquitin system in Huntington's disease. Nature *448*, 704–708.

Boone, D.L., Turer, E.E., Lee, E.G., Ahmad, R.C., Wheeler, M.T., Tsui, C., Hurley, P., Chien, M., Chai, S., Hitotsumatsu, O., et al. (2004). The ubiquitin-modifying enzyme A20 is required for termination of Toll-like receptor responses. Nat. Immunol. *5*, 1052–1060.

Conze, D.B., Wu, C.J., Thomas, J.A., Landstrom, A., and Ashwell, J.D. (2008). Lys63-linked polyubiquitination of IRAK-1 is required for interleukin-1 receptor- and toll-like receptor-mediated NF-kappaB activation. Mol. Cell. Biol. *28*, 3538–3547.

Cook, W.J., Jeffrey, L.C., Carson, M., Chen, Z., and Pickart, C.M. (1992). Structure of a diubiquitin conjugate and a model for interaction with ubiquitin conjugating enzyme (E2). J. Biol. Chem. *267*, 16467–16471.

Deng, L., Wang, C., Spencer, E., Yang, L., Braun, A., You, J., Slaughter, C., Pickart, C., and Chen, Z.J. (2000). Activation of the IkappaB kinase complex by TRAF6 requires a dimeric ubiquitin-conjugating enzyme complex and a unique polyubiquitin chain. Cell *103*, 351–361.

Ea, C.K., Deng, L., Xia, Z.P., Pineda, G., and Chen, Z.J. (2006). Activation of IKK by TNFalpha requires site-specific ubiquitination of RIP1 and polyubiquitin binding by NEMO. Mol. Cell *22*, 245–257.

Fellouse, F.A., Esaki, K., Birtalan, S., Raptis, D., Cancasci, V.J., Koide, A., Jhurani, P., Vasser, M., Wiesmann, C., Kossiakoff, A.A., et al. (2007). High-throughput generation of synthetic antibodies from highly functional minimalist phage-displayed libraries. J. Mol. Biol. *373*, 924–940.

Finley, D., Sadis, S., Monia, B.P., Boucher, P., Ecker, D.J., Crooke, S.T., and Chau, V. (1994). Inhibition of proteolysis and cell cycle progression in a multiubiquitination-deficient yeast mutant. Mol. Cell. Biol. *14*, 5501–5509.

Hayden, M.S., and Ghosh, S. (2008). Shared principles in NF-κB signaling. Cell *132*, 344–362.

Hershko, A., and Ciechanover, A. (1998). The ubiquitin system. Annu. Rev. Biochem. *67*, 425–479.

Kanakaraj, P., Schafer, P.H., Cavender, D.E., Wu, Y., Ngo, K., Grealish, P.F., Wadsworth, S.A., Peterson, P.A., Siekierka, J.J., Harris, C.A., and Fung-Leung, W.P. (1998). Interleukin (IL)-1 receptor-associated kinase (IRAK) requirement for optimal induction of multiple IL-1 signaling pathways and IL-6 production. J. Exp. Med. *187*, 2073–2079.

Kim, H.T., Kim, K.P., Lledias, F., Kisselev, A.F., Scaglione, K.M., Skowyra, D., Gygi, S.P., and Goldberg, A.L. (2007). Certain pairs of ubiquitin-conjugating enzymes (E2s) and ubiquitin-protein ligases (E3s) synthesize nondegradable forked ubiquitin chains containing all possible isopeptide linkages. J. Biol. Chem. *282*, 17375–17386.

Kirkpatrick, D.S., Hathaway, N.A., Hanna, J., Elsasser, S., Rush, J., Finley, D., King, R.W., and Gygi, S.P. (2006). Quantitative analysis of in vitro ubiquitinated cyclin B1 reveals complex chain topology. Nat. Cell Biol. *8*, 700–710.

Lee, C.V., Liang, W.C., Dennis, M.S., Eigenbrot, C., Sidhu, S.S., and Fuh, G. (2004a). High-affinity human antibodies from phage-displayed synthetic Fab libraries with a single framework scaffold. J. Mol. Biol. *340*, 1073–1093.

Lee, T.H., Shank, J., Cusson, N., and Kelliher, M.A. (2004b). The kinase activity of Rip1 is not required for tumor necrosis factor-alpha-induced IkappaB kinase or p38 MAP kinase activation or for the ubiquitination of Rip1 by Traf2. J. Biol. Chem. *279*, 33185–33191.

Legler, D.F., Micheau, O., Doucey, M.A., Tschopp, J., and Bron, C. (2003). Recruitment of TNF receptor 1 to lipid rafts is essential for TNFalpha-mediated NF-kappaB activation. Immunity *18*, 655–664.

Ordureau, A., Smith, H., Windheim, M., Peggie, M., Carrick, E., Morrice, N., and Cohen, P. (2008). The IRAK-catalysed activation of the E3 ligase function of Pellino isoforms induces the Lys63-linked polyubiquitination of IRAK1. Biochem. J. *409*, 43–52.

Peng, J., Schwartz, D., Elias, J.E., Thoreen, C.C., Cheng, D., Marsischky, G., Roelofs, J., Finley, D., and Gygi, S.P. (2003). A proteomics approach to understanding protein ubiquitination. Nat. Biotechnol. *21*, 921–926.

Pickart, C.M., and Raasi, S. (2005). Controlled synthesis of polyubiquitin chains. Methods Enzymol. *399*, 21–36.

Sato, S., Sanjo, H., Takeda, K., Ninomiya-Tsuji, J., Yamamoto, M., Kawai, T., Matsumoto, K., Takeuchi, O., and Akira, S. (2005). Essential function for the kinase TAK1 in innate and adaptive immune responses. Nat. Immunol. *6*, 1087–1095.

Sidhu, S.S., Lowman, H.B., Cunningham, B.C., and Wells, J.A. (2000). Phage display for selection of novel binding peptides. Methods Enzymol. *328*, 333–363.

Spence, J., Sadis, S., Haas, A.L., and Finley, D. (1995). A ubiquitin mutant with specific defects in DNA repair and multiubiquitination. Mol. Cell. Biol. *15*, 1265–1273.

Thomas, J.A., Allen, J.L., Tsen, M., Dubnicoff, T., Danao, J., Liao, X.C., Cao, Z., and Wasserman, S.A. (1999). Impaired cytokine signaling in mice lacking the IL-1 receptor-associated kinase. J. Immunol. *163*, 978–984.

Varadan, R., Walker, O., Pickart, C., and Fushman, D. (2002). Structural properties of polyubiquitin chains in solution. J. Mol. Biol. *324*, 637–647.

Wang, C., Deng, L., Hong, M., Akkaraju, G.R., Inoue, J., and Chen, Z.J. (2001). TAK1 is a ubiquitin-dependent kinase of MKK and IKK. Nature *412*, 346–351.

Wertz, I.E., O'Rourke, K.M., Zhou, H., Eby, M., Aravind, L., Seshagiri, S., Wu, P., Wiesmann, C., Baker, R., Boone, D.L., et al. (2004). De-ubiquitination and ubiquitin ligase domains of A20 downregulate NF-kappaB signalling. Nature *430*, 694–699.

Windheim, M., Stafford, M., Peggie, M., and Cohen, P. (2008). Interleukin-1 (IL-1) induces the Lys63-linked polyubiquitination of IL-1 receptor-associated kinase 1 to facilitate NEMO binding and the activation of IkappaBalpha kinase. Mol. Cell. Biol. *28*, 1783–1791.

Xiao, H., Qian, W., Staschke, K., Jiang, Z., Qian, Y., Cui, G., Deng, L., Chen, Z.J., Gilmour, R., and Li, X. (2008). Pellino 3b negatively regulates IL-1-indcued TAK1-dependent NF kappaB activation. J. Biol. Chem. *283*, 14654–14664.

Yamin, T.T., and Miller, D.K. (1997). The interleukin-1 receptor-associated kinase is degraded by proteasomes following its phosphorylation. J. Biol. Chem. *272*, 21540–21547.